Output-input ratio in thermally fluctuating biomolecular machines

Michal Kurzynski,[1,*] Mieczyslaw Torchala,[1,2] and Przemyslaw Chelminiak[1]
[1]*Faculty of Physics, A. Mickiewicz University, Umultowska 85, 61-614 Poznan, Poland*
[2]*BioInfoBank Institute, Limanowskiego 24A, 60-744 Poznan, Poland*
(Received 2 August 2013; revised manuscript received 15 September 2013; published 29 January 2014)

Biological molecular machines are proteins that operate under isothermal conditions and hence are referred to as free energy transducers. They can be formally considered as enzymes that simultaneously catalyze two chemical reactions: the free energy-donating (input) reaction and the free energy-accepting (output) one. Most if not all biologically active proteins display a slow stochastic dynamics of transitions between a variety of conformational substates composing their native state. This makes the description of the enzymatic reaction kinetics in terms of conventional rate constants insufficient. In the steady state, upon taking advantage of the assumption that each reaction proceeds through a single pair (the gate) of transition conformational substates of the enzyme-substrates complex, the degree of coupling between the output and the input reaction fluxes has been expressed in terms of the mean first-passage times on a conformational transition network between the distinguished substates. The theory is confronted with the results of random-walk simulations on the five-dimensional hypercube. The formal proof is given that, for single input and output gates, the output-input degree of coupling cannot exceed unity. As some experiments suggest such exceeding, looking for the conditions for increasing the degree of coupling value over unity challenges the theory. Performed simulations of random walks on several model networks involving more extended gates indicate that the case of the degree of coupling value higher than 1 is realized in a natural way on critical branching trees extended by long-range shortcuts. Such networks are scale-free and display the property of the small world. For short-range shortcuts, the networks are scale-free and fractal, representing a reasonable model for biomolecular machines displaying tight coupling, i.e., the degree of coupling equal exactly to unity. A hypothesis is stated that the protein conformational transition networks, as just as higher-level biological networks, the protein interaction network, and the metabolic network, have evolved in the process of self-organized criticality.

DOI: 10.1103/PhysRevE.89.012722 PACS number(s): 87.15.Ya, 05.70.Ln, 87.15.hp, 89.75.Hc

I. INTRODUCTION

The almost common conviction that biochemical processes can be interpreted in terms of conventional chemical kinetics is based on the assumption that the internal dynamics of biomolecules is fast enough to ensure the partial equilibrium state is reached before each kinetic step [1]. However, it has been clear for many years that this assumption cannot be true, as, in addition to fast vibrations, the dynamics of biomolecules also comprises slower stochastic transitions between a variety of conformational substates [2–5]. Research on biomolecular dynamics is being developed faster and faster, and a paradigm in which proteins need only a structure to function is more and more frequently extended to also involve dynamics [6–12]. Today, even in the case of small, water-soluble proteins, the "native state ensemble" [13–21] is talked about rather than a single native state, earlier identified with the protein tertiary structure, and, for very small proteins or protein fragments, trials to reconstruct the actual networks of conformational transitions are implemented [8,22–30]. Fischer's lock and key is presently replaced not by Koshland's induced fit but by the "conformational selection" concept [31–33]. The allosteric regulation appears to have a dynamic rather than a structural nature [31–37].

Because of the slow character of conformational dynamics, both the chemical and conformational transitions in an enzymatic protein have to be treated on an equal footing [5,38–40] and jointly described by a system of coupled master equations,

$$\dot{p}_l(t) = \sum_{l'} [w_{ll'} p_{l'}(t) - w_{l'l} p_l(t)], \tag{1}$$

determining the time variation of the occupation probabilities $p_l(t)$ of the individual protein's substates (Fig. 1). In Eq. (1), $w_{l'l}$ is the transition probability per unit time from the substate l to l', and the dot denotes the time derivative. The conformational transition probabilities satisfy the detailed balance condition, which, however, can be broken for the chemical transition probabilities controlled by the concentrations of the enzyme substrates.

In the closed reactor, the possibility that a chemical transformation will proceed before the conformational equilibrium has been reached results in the presence of a transient nonexponential stage of the process and in an essential dynamical correction to the reaction rate constant [1,2,16–18,38–40]. In the open reactor under stationary conditions (the concentrations of reactants and products of the reaction kept constant), the general situation is more complex. An analytical theory was proposed [5,41] only for the reactions gated by single pairs of transition conformational substates [Fig. 1(c)]. A consequence of the slow conformational transition dynamics is that the steady-state kinetics, like the transient stage kinetics, cannot be described in terms of usual rate constants. This possibility was suggested 40 years ago by Blumenfeld [42]. Later on still, we have shown that adequate physical quantities that should be used are the mean first-passage times between distinguished transition substates [5,41]. Thus, for

*kurzphys@amu.edu.pl

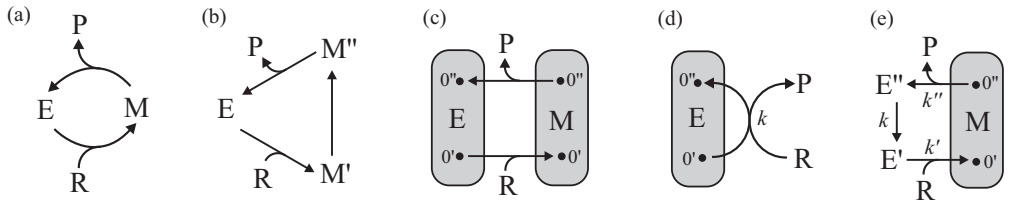

FIG. 1. Development of kinetic schemes of the single enzymatic reaction R ↔ P. (a) Two-step Michaelis-Menten kinetics, involving one enzyme-substrate intermediate M. (b) Three-step Haldene kinetics involving two intermediates. Here, M′ = ER and M″ = EP. (c) Kinetics studied in Ref. [41] where transitions between intermediates within E and M were expanded to networks of conformational transitions described by equations like (1) and represented here by the gray boxes. The reactant and product binding-releasing reactions are assumed to be gated, i.e., they take place only in certain conformational substates, represented here as black dots. (d) A simplified kinetic scheme including only the conformational transition dynamics within the free enzyme E. Two reactant and product binding-releasing reactions and the kinetics of the transitions within M are replaced by an effective single bimolecular reaction. (e) Simplified kinetic scheme including only the conformational transition dynamics within the enzyme-substrate complex M. All the reactions are reversible; the arrows indicate the directions assumed to be forward (the corresponding rate constants in the text are written with the subscript +).

the kinetic scheme shown in Fig. 1(c), the reciprocal forward turnover number appears to be a sum of the three times,

$$k_+^{-1} = \tau_{\mathrm{M}}(0' \to 0'') + (k_+'')^{-1} + \tau_{\mathrm{E}}(0'' \to 0'). \qquad (2)$$

The mean first passage time $\tau_{\mathrm{M}}(0' \to 0'')$ from the substate $0'$ to $0''$ characterizes a process of reaching the transition substate $0''$ in M, k_+'' is the equilibrium (transition state theory) reaction rate constant, and $\tau_{\mathrm{E}}(0'' \to 0')$ characterizes a process of the free enzyme-substrate molecular recognition.

An application of the formalism to two coupled enzymatic reactions was considered in the context of the free energy transduction in biological molecular machines [41]. We understand the word "machine" quite generally as denoting any physical system that enables two other physical systems to perform work one on each other. Under isothermal conditions, the performance of work is equivalent to a transduction of free energy. Thus, molecular machines that operate under such conditions are referred to as free energy transducers [43].

From a theoretical point of view, it is convenient to treat all biomolecular machines, also pumps and motors, as chemochemical machines. Indeed, the molecules present on either side of a biological membrane can be considered to occupy different chemical states, whereas the external load influences the free energy involved in binding the motor to its track, which can be expressed as a change of an effective concentration of this track [1]. The chemochemical machines are enzymes that simultaneously catalyze two chemical reactions: the free energy-donating (input) reaction and the free energy-accepting (output) reaction. For the chemochemical machines, the degree of coupling, i.e., the ratio of the output reaction flux to the input reaction flux, was also found to be determined by the mean first-passage times between the transition conformational substates. As the mean first-passage times are not the quantities that could be directly determined in the experiment, no experimental verification of the theory presented in Ref. [41] has been done as yet. The first goal of the present paper is to check the correctness of the theory by confronting it with the results of the Monte Carlo simulations, performed on the simple model networks of conformational transitions, and to introduce quantities that could be directly determined experimentally.

The essential motive of our studies is a trial to answer the intriguing question of whether it is possible for the degree of coupling to have a value higher than unity. A dogma in the physical theory of, e.g., biological molecular motors is the assumption that to take a single step along its track, the motor molecule has to hydrolyze at least one molecule of adenosine triphosphate (ATP). Several years ago this assumption was questioned by a group of Japanese biophysicists from the Yanagida laboratory, who, joining a specific nanometry technique with the microscopy fluorescence spectroscopy, showed that the myosin II head can take several steps along the actin filament per ATP molecule hydrolyzed [44–46]. This observation has been confirmed by other laboratories [47], and also for the cytoplasmic dynein [48–51].

No conventional chemical kinetics approach is able to explain such behavior. In Refs. [41] and [1], based on approximations carried too far, we suggested that the degree of coupling can exceed unity already for reactions proceeding through single pairs of transition substates. Here, we formally prove that it is not the case, and we show that the latter takes place in a natural way for the scale-free critical branching trees extended by long-range shortcuts, and with the output gates involving more conformational substates.

II. GENERALIZED KINETIC SCHEME OF CHEMOCHEMICAL MACHINE ACTION

The principle of the action of the chemochemical machine is simple [43]. It is a protein enzyme that catalyzes simultaneously two chemical reactions [Fig. 2(a)]. Separately, each reaction takes place in the direction determined by the second law of thermodynamics stating that the energy dissipated, determined by the product of flux and force, is positive. However, if both reactions take place simultaneously in a common cycle, they must proceed in the same direction, and the direction of the first reaction can force a change of direction in the second. As a consequence, the first reaction transfers a part of its free energy, recovered from dissipation, for performing work on the second reaction.

In formal terms, the chemochemical machine couples two unimolecular reactions: the free energy-donating reaction $R_1 \leftrightarrow P_1$ and the free energy-accepting reaction $R_2 \leftrightarrow P_2$.

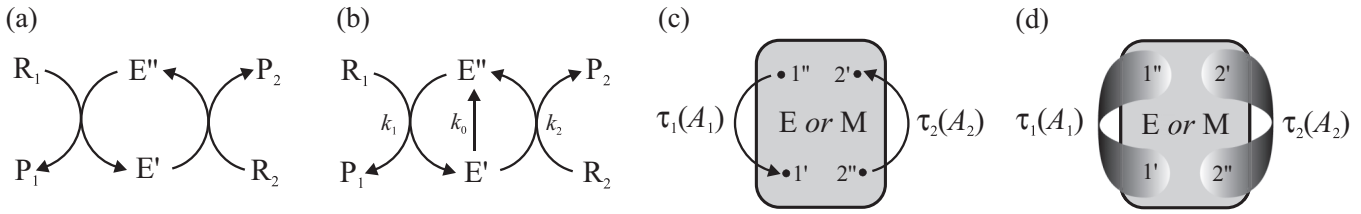

FIG. 2. Development of kinetic schemes of the chemochemical machine. (a) The principle of the chemochemical free energy transduction. Due to proceeding on the same enzyme, reaction $R_1 \leftrightarrow P_1$ drives reaction $R_2 \leftrightarrow P_2$ against its conjugate force, determined by steady-state concentrations of the product $[P_2]$ and the reactant $[R_2]$. (b) Assumption of a possible short circuit or slippage of the input vs output reaction. (c) Assumption of both the free energy-donating and the free energy-accepting reaction to participate in a kinetic scheme such as the one shown in Fig. 1(d) or 1(e). $\tau_1(A_1)$ and $\tau_2(A_2)$ denote, respectively, the mean input and output external transition times in the forward direction, dependent on the concentrations $[R_i]$ and $[P_i]$, and thus the forces A_i [cf. Eqs. (9) or (10)]. (d) Further generalization of the kinetic scheme to involve more input and output gates.

Bimolecular reactions can be considered as effective unimolecular reactions upon assuming a constant concentration of one of the reagents, e.g., adenosine diphosphate (ADP) in the case of ATP hydrolysis. The input and output fluxes J_i ($i = 1$ and 2, respectively) and the conjugate thermodynamic forces A_i are defined as [43]

$$J_i = \frac{d[\mathrm{P}_i]/dt}{[\mathrm{E}]_0} \tag{3}$$

and

$$\beta A_i = \ln K_i \frac{[\mathrm{R}_i]}{[\mathrm{P}_i]}, \quad K_i \equiv \frac{[\mathrm{P}_i]^{\mathrm{eq}}}{[\mathrm{R}_i]^{\mathrm{eq}}}. \tag{4}$$

Here, the symbols of the chemical compounds in the square brackets denote the molar concentrations in the steady state (no superscript) or in the equilibrium (the superscript "eq"). $[\mathrm{E}]_0$ is the total concentration of the enzyme and β is proportional to the reciprocal temperature, $\beta \equiv (k_\mathrm{B}T)^{-1}$, where k_B is the Boltzmann constant.

The flux-force dependence is one-to-one only if some constraints are put on the concentrations $[\mathrm{R}_i]$ and $[\mathrm{P}_i]$ for each i. There are two options. Either the concentration of one species, say R_i, in the open reactor under consideration, is kept constant:

$$[\mathrm{R}_i] = \mathrm{const} \tag{5}$$

as, e.g., in the case of ATP hydrolysis, or it is a total concentration of the enzyme substrate:

$$[\mathrm{R_i}] + [\mathrm{P}_i] = \mathrm{const}, \tag{6}$$

as, e.g., in the case of a motor motion, where $[\mathrm{R}_i]$ and $[\mathrm{P}_i]$ are interpreted as the effective concentrations of its track before and after translation, respectively [1].

The free energy transduction is realized if the product J_2A_2, representing the output power, is negative. The efficiency of the machine is the ratio

$$\eta = -J_2A_2/J_1A_1 \tag{7}$$

of the positive output power to the input power. In general, the degree of coupling

$$\epsilon = J_2/J_1, \tag{8}$$

being itself a function of the forces A_1 and A_2, can be both positive and negative.

Usually, the assumption of tight coupling between both reactions is made [Fig. 2(a)]. It states that the flux of the first reaction equals the flux of the second, $J_1 = J_2$, thus $\epsilon = 1$. However, an additional reaction can take place between the two states E′ and E″ of the enzyme [Fig. 2(b)]. The latter reaction can be considered either as a short circuit (the nonproductive realization of the first reaction not driving the second reaction) or a slippage (the realization of the second reaction in the direction dictated by its conjugate force).

The multiconformational counterpart of the scheme in Fig. 2(b) is shown in Fig. 2(c). Here, as in the scheme in Fig. 1(d), a network of conformational transitions within the enzyme is represented by the gray box, and the assumption of gating by single pairs of transition conformational substates is made. The gray box in Fig. 2(c) can also represent a network of conformational transitions within the enzyme-substrate or enzyme-substrates complex, shown in the scheme in Fig. 1(e). The only difference consists in the dependence of the mean transition times τ_i in the forward direction, between the gate substates i'' and i' ($i = 1,2$), on $[\mathrm{R}_i]$ and $[\mathrm{P}_i]$, thus the external forces A_i. For the effective single bimolecular reaction in the scheme in Fig. 1(d) (the interior of the gray box represents the substates of E),

$$\tau = \frac{1}{k_+[\mathrm{R}]}, \tag{9}$$

whereas for the three successive effective reactions in the scheme in Fig. 1(e) (the interior of the gray box represents the substates of M),

$$\tau = \frac{1}{k''_+} + \frac{k''_-[\mathrm{P}]}{k''_+}\left(\frac{1}{k_+} + \frac{k_-}{k_+}\frac{1}{k'_+[\mathrm{R}]}\right). \tag{10}$$

Together with the equilibrium occupation probabilities of the forward transition substates [doubly primed in Fig. 2(c)], the mean transition times τ_i determine the external transition probabilities per unit time,

$$v_{i'i''} = \left(\tau_i\, p^{\mathrm{eq}}_{i''}\right)^{-1}. \tag{11}$$

We denote the external transition probabilities by v to distinguish them from possible internal transition probabilities between the same substates, denoted by w. The external transition probabilities per unit time from the transition substates in the reverse direction [singly primed in Fig. 2(c)] must be multiplied by the factor breaking the detailed balance

symmetry, determined by the external forces:

$$v_{i''i'} = e^{-\beta A_i}\left(\tau_i p_{i'}^{\mathrm{eq}}\right)^{-1}. \tag{12}$$

In Ref. [41], using a technique of summing up the directional diagrams proposed by Hill [43], who formalized a former idea of Kirchhoff's, we showed how the input and the output reaction fluxes are related to the mean first-passage times between the distinguished substates. In the next section, we quote the most important results of Ref. [41] in the essentially changed notation facilitating their experimental verification. Further on, we compare them with the results of the random-walk simulations on a simple model network. The relations between the stationary fluxes and mean first-passage times are explained briefly in the Appendix.

Using the relations derived in the Appendix, we formally prove that, for the scheme in Fig. 2(c), the degree of coupling (8) cannot exceed unity. To obtain a higher value of this coefficient, an extension of the transition gates is necessary, which is schematically shown in Fig. 2(d). The rate of the external transition within each component subgate can differ one from another, so that such kinds of models are referred to as models with "fluctuating barriers" [5]. The fact that extensions of the output gates really result in exceeding the value of the degree of coupling over unity is shown in the final section.

III. SINGLY GATED REACTIONS: THEORETICAL RESULTS

For all the schemes shown in Figs. 2(a)–2(c), the flux-force dependence for the two coupled reactions has a general functional form [41],

$$J_i = \frac{1 - e^{-\beta(A_i - A_i^{\mathrm{st}})}}{J_{+i}^{-1} + J_{-i}^{-1} e^{-\beta(A_i - A_i^{\mathrm{st}})} + J_{0i}^{-1}(K_i + e^{\beta A_i})^{-1}}. \tag{13}$$

The parameters J_{+i}, J_{-i}, J_{0i}, and A_i^{st} depend on the other force and are determined by a particular kinetic scheme. A_i^{st} have the meaning of stalling forces for which the fluxes J_i vanish: $J_i(A_i^{\mathrm{st}}) = 0$. The dependences $J_i(A_i)$ are strictly increasing with an inflection point, determined by J_{0i}, and two asymptotes, J_{+i} and J_{-i} (cf. Fig. 4). The asymptotic fluxes J_{+i} and J_{-i} display the Michaelis-Menten dependence on the substrate concentrations. Because of the high complexity, we refrain from giving any formulas for the turnover numbers and the apparent dissociation constants.

The degree of coupling dependence on the forces A_1 and A_2 has a form

$$\epsilon = \frac{1 - e^{-\beta(A_1+A_2)} + W_1(A_1)(1 - e^{-\beta A_2})}{1 - e^{-\beta(A_1+A_2)} + W_2(A_2)(1 - e^{-\beta A_1})} \tag{14}$$

and the stalling force,

$$\beta A_2^{\mathrm{st}} = \ln \frac{e^{-\beta A_1} + W_1(A_1)}{1 + W_1(A_1)}. \tag{15}$$

The expression for A_1^{st} is to be obtained after replacing the index 1 with the index 2 and vice versa. The quantities $W_i(A_i)$ are measures of the slippage. To facilitate their interpretation by the reader, we adduce the corresponding formulas for the simple scheme shown in Fig. 2(b) [1]:

$$W_1(A_1) = k_{0-}\tau_1, \quad W_2(A_2) = k_{0+}\tau_2, \tag{16}$$

where τ_i are determined by Eq. (9) both for R_1 and R_2. To express it more directly, $W_i(A_i)$ can be considered as representing the ratios of nonproductive and productive transition rates.

For the scheme in Fig. 2(c), the summation over diagrams gives [41]

$$W_1(A_1) = \frac{\tau_{\mathrm{M}}(1'' \leftrightarrow \{1',2'\}) + \tau_{\mathrm{M}}(1' \leftrightarrow \{1'',2''\})e^{-\beta A_1} + \tau_1(A_1)}{\tau_{\mathrm{M}}(1' \leftrightarrow \{1'',2'\}) - \tau_{\mathrm{M}}(1' \leftrightarrow \{1'',2''\})} \tag{17}$$

and the equivalent for $W_2(A_2)$ after replacing 1 with 2 and vice versa [note the 180° rotational symmetry of the kinetic scheme in Fig. 2(c)].

The quantities τ_{M} in Eq. (17) denote the sums

$$\tau_{\mathrm{M}}(l_0 \leftrightarrow \{l,l'\}) = \tau_{\mathrm{M}}(l_0 \to \{l,l'\}) + \tau_{\mathrm{M}}(\{l,l'\} \to l_0) \tag{18}$$

of the forward and reverse mean first-passage times that occur in the summation formula for the mean first-passage time from l_0 to l in the network symbolized by the gray box M:

$$\tau_{\mathrm{M}}(l_0 \to l) = \tau_{\mathrm{M}}(l_0 \to \{l,l'\}) + \tau_{\mathrm{M}}(\{l_0,l'\} \to l) \tag{19}$$

for arbitrary l' (cf. the Appendix). Equation (19) is a generalization of the obvious summation formula for a one-dimensional random walk:

$$\tau(l_0 \to l) = \tau(l_0 \to l') + \tau(l' \to l), \tag{20}$$

where l' lies between l_0 and l. The quantity $\tau_{\mathrm{M}}(l_0 \to \{l,l'\})$ has a direct meaning of the mean first-passage time from l_0 to l *or* l'. The interpretation of $\tau_{\mathrm{M}}(\{l_0,l'\} \to l)$ is more troublesome, but it can always be treated as a completion of $\tau_{\mathrm{M}}(l_0 \to \{l,l'\})$ to $\tau_{\mathrm{M}}(l_0 \to l)$. On doing so, we find

$$\tau_{\mathrm{M}}(l_0 \leftrightarrow \{l,l'\}) = \tau_{\mathrm{M}}(l_0 \to \{l,l'\}) - \tau_{\mathrm{M}}(l \to \{l_0,l'\}) + \tau_{\mathrm{M}}(l \to l_0). \tag{21}$$

We get an alternative expression upon exchanging l with l'.

The highest value of the degree of coupling modulus $|\epsilon|$ in the free energy transduction region is for $\beta A_2 = 0$. Then, Eq. (14) is simplified to

$$\epsilon(0) = \frac{1}{1 + W_2(0)} \tag{22}$$

independently of βA_1, and

$$\beta A_1^{\mathrm{st}}(0) = 0. \tag{23}$$

One could expect the value of $|\epsilon|$ to be higher than 1 if $W_2(0)$ was negative, i.e., if the denominator in the equation symmetrical to (17) was negative. However, this is not the case. It is worth pointing out that the denominators in $W_1(A_1)$ and $W_2(A_2)$ equal each other. This follows from the relation (A12) derived in the Appendix. The consequence is that both $W_i(A_i)$ are always of the same sign, either positive or negative. If both W_i are positive, the stalling force βA_2^{st} given by Eq. (15) is negative and the free energy transduction takes place in the region $A_2^{\mathrm{st}} \leqslant A_2 \leqslant 0$ with the positive value of the degree of coupling (22) always lower than unity.

If both W_i are negative, the stalling force βA_2^{st} given by Eq. (15) is positive and the free energy transduction takes

place in the region $0 \leqslant A_2 \leqslant A_2^{\rm st}$ with the negative ϵ. For its value to be lower than -1, an inequality

$$-2 < W_2(0) < -1 \tag{24}$$

should be fulfilled. Upon substituting the explicit expression for $W_2(0)$ and using the relation (A10), also derived in the Appendix, this inequality can be rewritten as

$$\tau_{\rm M}(2' \leftrightarrow \{1'',2''\}) + \tau_{\rm M}(2'' \leftrightarrow \{1'',2'\}) + \tau_2(0) < 0. \tag{25}$$

Of course, neither $\tau_{\rm M}$ nor τ_2 can be negative, so the modulus of the coupling ratio can never be higher than unity.

IV. SINGLY GATED REACTIONS: COMPARISON WITH MONTE CARLO SIMULATIONS

The quantities $\tau_{\rm M}(l_0 \leftrightarrow \{l,l'\})$ or their differences occurring in Eq. (17) for $W_1(A_1)$ and the equivalent for $W_2(A_2)$ can be considered as five independent parameters of the theory to be fitted in future experiments. However, the mean first-passage times are not the quantities that could be directly determined experimentally. The choice of an appropriate network that models the interior of the gray box in Fig. 2(c) and the positions of the input and output gates is a question of the statement of a more or less reasonable hypothesis. The simplest was stated 70 years ago by Kramers, who assumed that the slowly varying intramolecular substates lie along a one-dimensional "reaction coordinate" [1,2]. This way of reasoning has been continued in the theory of molecular motors where the reaction coordinate was identified with the position of the motor along its track [43,52–54] or the rotation angle [55].

More complex modeling can be grounded on statistical analyses of the time series found in molecular-dynamics simulations [8,22–30] or single-molecule experiments [56–64]. Unfortunately, the present-day understanding of this matter is still rather poor, so we decided, first, to test our theory by resorting to Monte Carlo simulations of random walks on simple but not quite real networks. Various networks differ from one another by the geometry of links that determines an entropic contribution to the kinetics, and by the variety and asymmetry of the transition probabilities $w_{ll'}$ that, following the detailed balance condition, determine an energetic contribution.

To start with, for more detailed studies, we chose the most regular isoenergetic network, the n-dimensional hypercube, the vertexes of which are labeled by sequences of the bits $(s_1,s_2,\ldots,s_n)$, $s_i = 0,1$, and all possible transitions are related to changes of one bit and have the same probability w. The distance between vertexes is determined by the minimum number of edges a random walker has to pass in a walk between these vertexes. Such a determined distance equals the number of necessary bit changes. In the n-dimensional hypercube, there are $N = 2^n$ vertexes. Each vertex has n neighbors, and no boundary conditions are necessary. To obtain the results of simulations in a reasonable amount of time, we assumed the dimension to be $n = 5$.

We chose the input and output gates so as to make the free energy transduction the most effective. It is realized when moduli of both the degree of coupling (14) and the stalling force (15) are maximum, i.e., the values of $W_2(0)$ and $W_1(\infty)$ are minimum. A detailed analysis indicated that it takes place when the pairs of sites $1'$ and $2''$ as well as $2'$ and $1''$ lie closest, at a distance equal to 1. On the contrary, the diameters of the input and output gates should be the largest, equal to 5 so as to lie along the diagonal of the hypercube.

For such determined geometry of the gates, only the values of the three types of mean first-passage times have to be known, enabling one to calculate, following Eq. (21), all the quantities occurring in Eq. (17) for $W_1(A_1)$ and the equavalent for $W_2(A_2)$. These are mean first-passage times of the type

$$\begin{aligned}\tau_{\rm M}(1'' \to \{1',2'\}) &= 16,\\ \tau_{\rm M}(1' \to \{1'',2'\}) &= 80/3 \approx 26.667,\\ \tau_{\rm M}(1' \to 1'') &= 128/3 \approx 42.667\end{aligned}$$

(note that for the hypercube, the mean first-passage times depend only on the distances between the initial, final, and the intermediate, if any, states). All the quoted values, counted in the number of random-walk steps with the transition probability between the nearest neighbors $w = 1/n = 1/5$, were determined by simple though time-consuming combinatorics and checked in numerical simulations.

The reciprocal external transition times equal the equilibrium occupation probabilities of the transition gates $1/N = 1/2^n = 1/32$ multiplied by appropriate external transition rates, Eq. (11). We assumed the simplest, constant external transition rates and chose $\tau_1^{-1} = 50\,w/N = 5/16$ and $\tau_2^{-1} = 30\,w/N = 3/16$. The times $\tau_1 = 3.200$ and $\tau_2 = 5.333$ are one order of magnitude shorter than the maximum mean first-passage time $\tau_{\rm M}(1' \to 1'')$, being a measure of the intramolecular relaxation time. Thus, both reactions 1 and 2 are controlled, though not completely, by intramolecular dynamics. In fact, shortening the times τ_1 and τ_2 does not change the values of W_1 and W_2 considerably. Following Eq. (12), the reciprocal reverse external transition times equal τ_1^{-1} and τ_2^{-1} multiplied by the detailed equilibrium condition-breaking exponents $\exp(-\beta A_1)$ and $\exp(-\beta A_2)$, respectively. We chose $\beta A_1 = 10$, which is a physically reasonable condition of the free energy donating reaction 1 to proceed sufficiently far from the equilibrium. In actual simulations, to preserve the equal probabilities of the forward and reverse internal transitions in the presence of additional external transitions, w had to be chosen much lower than $1/n$, and a high probability of waiting at all but one vertex had to be added.

A typical result of a simulation of the time course of the net number of external transitions through the input and the output gates is shown in Fig. 3(a). It is clearly seen that, even for such a small lattice studied, consisting of 32 vertexes, large fluctuations make the determination of the input and the output fluxes in 10^4 iteration steps impossible. Only by increasing the number of iteration steps to 10^9 [Fig. 3(b)] can one determine the fluxes with the error lower than 0.3%.

The theory presented in the previous section, in particular its main Eqs. (14), (15), and (17), does not use any approximation and is exact. For simple networks of conformational transitions such as the one considered here, we know the values of appropriate mean first-passage times and we can directly compute the slippage functions $W_i(A_i)$, and thus the force dependences of the degree of coupling (14) and the stalling

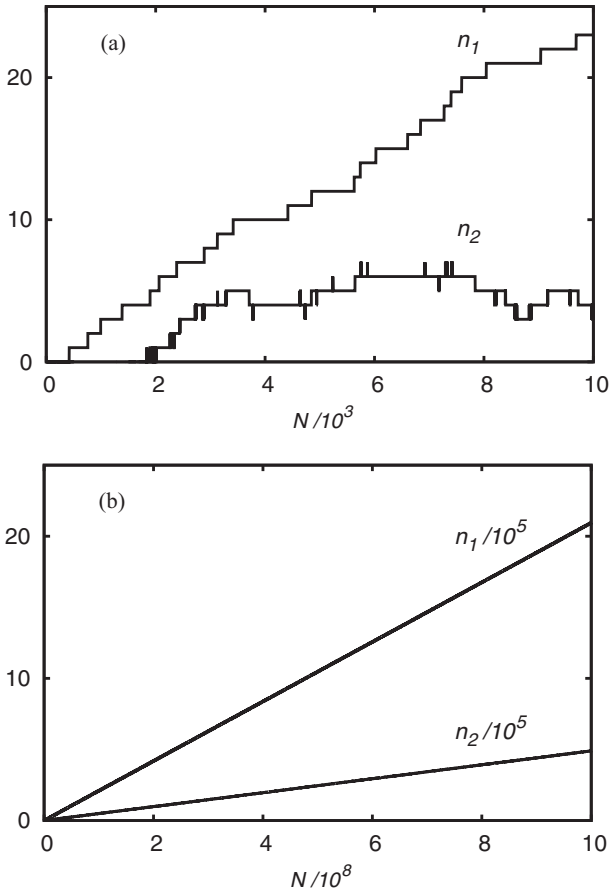

FIG. 3. Simulated time course of the net number of the input ($R_1 \leftrightarrow P_1$) and the output ($R_2 \leftrightarrow P_2$) external transitions for the five-dimensional hypercube with the gates and the parameters described in the text. (a) The snapshots made every step. (b) The snapshots made every 10^5 steps.

force (15). Figures 4 and 5 show the confrontations of such obtained dependences with the results of the Monte Carlo simulations, which, in the present context, can be treated as experimental data. Note that $\epsilon(0) = 0.28$. Taking into account that in Figs. 4 and 5 no fitting procedures were applied, the agreement is excellent, but it only points to the correctness of the conditions under which our Monte Carlo simulations were performed. Being sure of such correctness, we can use similar simulations to study more extended networks for which no exact theory exists.

V. MULTIPLY GATED REACTIONS: ISOENERGETIC NETWORK MODELS

We proved the theorem that the value of the degree of coupling was lower than, or at the most equal to, unity, but only when the input and output reactions proceeded through single pairs of transition conformational substates. It is reasonable to suppose that the chance of a higher degree of coupling is possible if the output gate is extended to two or more pairs of transition substates. In fact, it is obvious that, upon replacing the single output gate in the scheme in Fig. 2(a) by n gates succeeding each other, we get the degree of coupling $\epsilon = n$. Such reasoning has already been proposed in order to explain

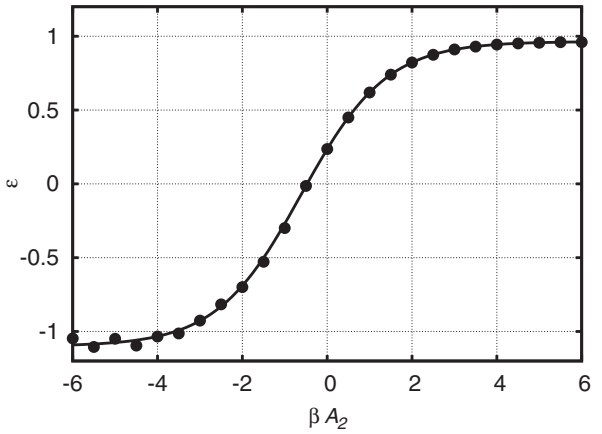

FIG. 4. Dependence of the degree of coupling ϵ on the output force A_2 for the model and the parameters described in the text. The black dots denote the results of the Monte Carlo simulations and the continuous line is calculated following Eqs. (14), (17) and the equivalent for $W_2(A_2)$. No fit has been performed between the experiment and the theory, as the latter has no free parameters. As for the very high value of the input force $\beta A_1 = 10$, the input flux J_1 remains practically constant, the figure simultaneously represents the dependence of the output flux $J_2 = \epsilon J_1$ on the output force A_2. In fact, the results of our Monte Carlo experiment fit the more general theoretical prediction, Eq. (13), very well.

the multiple stepping of the myosin molecule along the actin filament [45]. One can also imagine an incorporation of a system of additional nonreactive transitions [65].

In Fig. 6, a scheme is shown with one input and two output gates, being an extension of the kinetic scheme in Fig. 2(c). Unfortunately, even in the case of only two output gates, the analytical formulas are so complex and not transparent that serious approximations must be made from the very beginning. Not being able presently to formulate such approximations, we decided to apply a computer experiment for a preliminary study of the problem. We performed Monte Carlo simulations starting from the five-dimensional hypercube. For the most

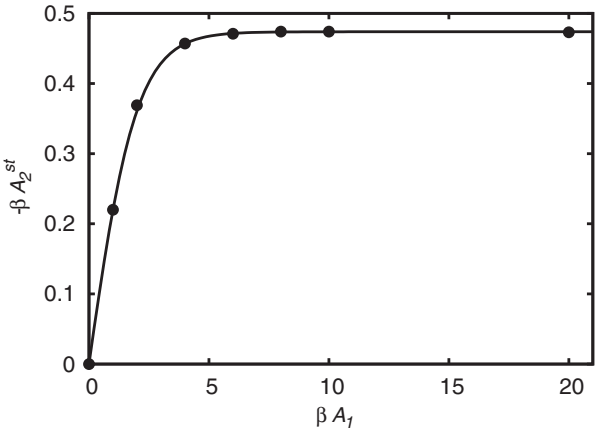

FIG. 5. Dependence of the stalling force A_2^{st} on the input force A_1 for the model and the parameters described in the text. The black dots denote the results of the Monte Carlo simulations and the continuous line is calculated following Eqs. (15) and (17).

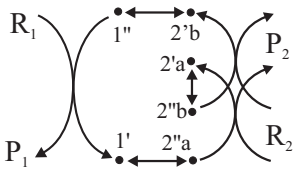

FIG. 6. Extension of the kinetic scheme in Fig. 2(c) to one input and two output gates. The obligatory transitions are drawn by arrows. If no other transitions occur, the degree of coupling between the second and the first reaction equals 2. Otherwise, it is lower than 2, but possibly higher than 1.

optimal geometry of one input and two output gates, we obtained the degree of coupling $\epsilon(0)$ not higher than 0.36. Also, simulations on the nine-dimensional hypercube with 512 states were not successful. We suppose that the input and output steady-state fluxes on the isoenergetic hypercubes of an arbitrary dimension and with an arbitrary number of gates are always equal to the steady-state fluxes through the single input and output gates on some equivalent nonisoenergetic networks. Such systems are described by the theory given above, and the whole discussion already performed applies to them.

Still restricting ourselves to isoenergetic networks, we considered systems with a more complex topology. We focused our attention on networks with a hierarchy of bottlenecks or dead ends, the diffusion on which displays long-time tiles [66]. As an example of a network with a hierarchy of bottlenecks, we considered the Sierpinski gasket; as an example of a network with a hierarchy of dead ends, we considered the Bethe lattice. As in Sec. IV, we assumed short external transition times and the large input force $\beta A_1 = 10$. For the Sierpinski gasket of the fourth order with the most optimal system of three successive gates, we obtained $\epsilon(0) = 1.27$. For the Bethe lattice with five shells and the most optimal system of three successive gates, we obtained $\epsilon(0) = 1.19$. We conclude that for protein machines with stochastic dynamics described by an appropriate network of conformational transitions, the degree of coupling can, in principle, be higher than unity.

The most optimal geometry of gates is the one with a bias against unfavorable short circuits and, simultaneously, long wandering between transitions through successive gates. However, this goal was achieved in an evidently artificial way due to entropic obstacles and shortcuts. The values of ϵ obtained were much lower than the maximal possible value 3. Similarly, the value $\epsilon(0) = 0.28$, obtained for the five-dimensional cube with the most optimal single output gate, was much lower than the maximal possible value 1 detected experimentally for numerous tightly coupled biomolecular machines. The conclusion follows that the isoenergetic networks considered up to now are not good models of conformational transition networks in real native proteins, and there is a need to look for more realistic models.

VI. MULTIPLY GATED REACTIONS: CRITICAL BRANCHING TREE MODELS

Since the formulation by Bak and Sneppen of the cellular automaton model of the Eldredge and Gould punctuated equilibriums [67], biological evolution is more and more often considered to be a self-organized criticality phenomenon [68,69]. An evolving network model of self-organized criticality was proposed by Barabási and Albert [70,71]. It soon appeared that two networks of the systems biology, namely the protein interaction network and the metabolic network, to a good approximation, not only have a scale-free structure like that of the Barabási-Albert networks [72,73], but they also display a fractal scaling [74,75].

There are grounds to also suppose that the conformational transition networks in proteins are both scale-free and fractal. The former feature is suggested by the results of the molecular dynamics simulations for small atomic clusters [76] and proteins as well [77], and by a specific spatial organization of proteins [78,79]. The latter has already been shown in the pioneering papers from the Hans Frauenfelder laboratory [2,6] and confirmed in early molecular dynamics simulations [3,4]. Thus, it is a reasonable hypothesis that the protein conformational transition networks have also evolved in a process of self-organized criticality.

However, the above speculations are somewhat incomplete. The evolving scale-free Barabási-Albert networks evidently have small-world character rather than fractal character [71]. And indeed, such a character was also suggested both for the protein interaction network and the metabolic network [80], as well as for the conformational transition networks [76,77]. Only recently has an apparent contradiction between fractality and small-worldness been explained by the application of the renormalization-group technique [81]. It appears that, upon adding shortcuts with the distance r distribution fulfilling the power law $r^{-\alpha}$ to an original fractal network, a transition to the small-world network occurs below some critical value of the exponent α. Close to this critical value, the network can be fractal in a small length-scale while simultaneously having small-world features in a large length-scale, and this is the case of the protein interaction network and the metabolic network. The small-world properties of the conformational transition network have been shown for a protein that has experienced a folding transition [77], whereas the fractal hierarchy characterizes the well-folded proteins [3,4,29]. We can suppose that for partly unfolded proteins, the conformational transition network also displays fractal properties on a small length-scale and small-world properties on a large length-scale [82].

The topological structure of a flow (of probability, metabolites, energy, or information) through a network is characterized by a spatial spanning tree composed of the most conducting links not involved in cycles. It is referred to as the skeleton [83] or the backbone [84] of the network, all the rejected links being considered as shortcuts. The skeleton of the scale-free and fractal network is also scale-free and fractal. For the scale-free fractal trees, a criticality feature appears important that denotes the presence of a plateau equal to unity in the mean branching number dependence on the distance from the skeleton root. The critical trees can be completed for self-similar scale-free networks, and such is the case of the protein interaction and metabolic networks [83,85].

Figure 7(a) shows a tree with $N = 200$ nodes constructed following the algorithm described in Ref. [83]. It is too small to prove its scale-free and fractal properties, but the same algorithm applied to $N = 10^5$ nodes resulted in a tree being actually critical, scale-free, and fractal. The important feature

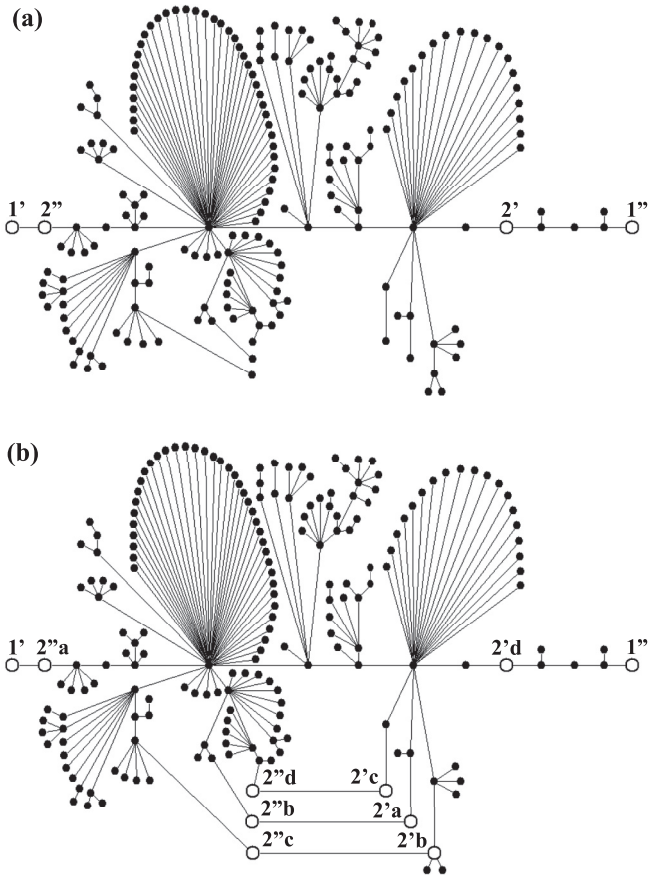

FIG. 7. (a) Exemplifying realization of a scale-free fractal tree with $N = 200$ nodes constructed following the algorithm described in Ref. [83]. The single input and output gates are distinguished, chosen for the Monte Carlo simulations. For notation of the gates, see Fig. 2(c). (b) Tree from the upper figure, extended by three randomly chosen shortcuts between pairs of nodes equally distanced from the two main hubs. The four output gates a, b, c, and d are chosen tendentiously to lie one after the other as in Fig. 6, hence to obtain the highest value of the degree of coupling ϵ.

of the scale-free fractal trees is the repulsion of the hubs (the nodes with a large number of links) [83]. And, indeed, for most protein conformational networks, a tree joining two main states, e.g., closed and open ones, is characteristic [27–30].

Figure 7(b) shows an extension of the tree from Fig. 7(a) by three randomly chosen shortcuts between pairs of nodes equally distanced from the two main hubs. And again, this network is too small to determine its scaling properties, but a similar procedure applied to the scale-free and fractal tree with $N = 10^5$ nodes results in a network that is fractal in a small length-scale and small-world in a large length-scale.

To provide both networks with stochastic dynamics described by Eq. (1), we assume the probability of changing a node to any of its neighbors to be the same in each random-walk step. Consequently, the transition probability from the node l to the neighboring node l' is

$$w_{l'l} = 1/k_l, \tag{26}$$

where k_l is the number of links (the degree) of the node l. A network with such dynamics cannot be isoenergetic, and, following the detailed balance principle, the equilibrium occupation probability of the node l is

$$p_l^{\mathrm{eq}} = k_l \Big/ \sum_{l'} k_{l'}. \tag{27}$$

The larger the number of links, the higher the equilibrium occupation probability of the node, thus the lower its free energy. The most stable conformational substates are the hubs.

As in Secs. IV and V, we choose the simplest, constant external transition times τ_1 and τ_2 for the input and output gates, respectively, related to Eq. (9) and the constraint (5). We also choose $\beta A_1 = 10$, which makes the exit probability from the transition substate $1'$ negligible. Following Eq. (27), the internal transition probabilities per unit time (26) can be rewritten in a form similar to (11):

$$w_{l'l} = \left(\tau_{\mathrm{rx}} p_l^{\mathrm{eq}}\right)^{-1}, \tag{28}$$

where

$$\tau_{\mathrm{rx}} = \sum_l k_l \tag{29}$$

denotes the intramolecular relaxation time.

To ensure that the sum of all transition probabilities from a given node will be 1 in the actual simulation step, all the discussed transition probabilities were appropriately renormalized with a probability of waiting at all but one nodes added.

The repulsion of the main hubs results in the long mean first-passage times between them. As a consequence, intramolecular dynamics of this type can easily explain the tight coupling between the output and input reaction for most protein machines. For the system of chosen gates as shown in Fig. 7(a), we performed a series of Monte Carlo simulations and found $\epsilon(0) = 0.988$ for $\tau_1 = \tau_2 = 40$, those times being one order of the magnitude shorter than $\tau_{\mathrm{rx}} = 400$, and $\epsilon(0) = 0.998$ for $\tau_1 = \tau_2 = 4$. This means that the times $\tau_1 = \tau_2 = 40$ are short enough to almost reach the maximum degree of coupling.

The case of multiple output gates requires more systematic studies. Upon tendentiously choosing the four output gates a, b, c, and d as shown in Fig. 7(b) and assuming $\tau_1 = \tau_2 = 40$, we found $\epsilon(0) = 2.27$, a value much closer to the the maximum value possible $\epsilon(0) = 4$ than in the case of isoenergetic networks. We also performed simulations for nonzero values of the force A_2, and we obtained a dependence $\epsilon(A_2)$ shown in Fig. 8. We tried to fit the results of the Monte Carlo simulations to Eq. (13), but our success does not necessarily mean that this equation is universal and applies also to the multiply gated reactions. It simply contains a sufficient number of parameters.

The curve in Fig. 8 is concave. Upon changing the geometry of the gates and, possibly, taking into account a variation of τ_2 with A_2 and with a particular index of the output gate (the "fluctuating barrier"), one can obtain the convex dependences $\epsilon(A_2)$ or $J_2(A_2)$, well known in the case of the actomyosin motor [41].

A more serious limitation of the present model is the assumption of constancy of transition probabilities for a given degree of the node, Eq. (26). It gives only a trivial dependence on temperature and does not provide a funnel-like change of the network architecture, characterizing the process of protein

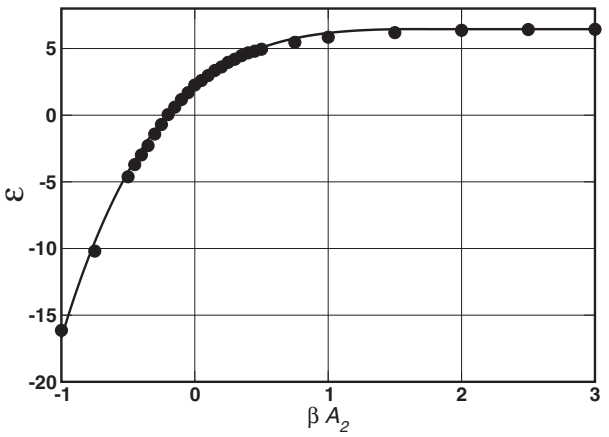

FIG. 8. Dependence of the degree of coupling ϵ on the output force A_2 for the model with four gates, presented in Fig. 7(b). The black dots denote the results of the Monte Carlo simulations and the continuous line represents the fit to Eq. (13). The free energy transduction region is characterized by the parameters $\epsilon(0) = 2.27$ and $\beta A_2^{\rm st} = -0.21$.

folding [23]. Because of the number of parameters needed for a more systematic analysis, we leave the problem of possible model extensions to a separate paper devoted to a particular theory of the actomyosin motor.

VII. CONCLUDING REMARKS

Only recently have some trials been undertaken to determine the conformational transition networks in native proteins. That is why in the present paper we restricted our attention to model networks. Our goal was to calculate and simulate the degree of coupling between the free energy-accepting and the free energy-donating reaction flux in the protein molecular machines. Exact theoretical formulas could be obtained only for the reactions proceeding through single pairs (the gates) of conformational transition substates. The theory predicts the value of the degree of coupling not exceeding unity. However, in Monte Carlo simulations on simple scale-free treelike networks extended by long-range shortcuts, we show that, upon increasing the number of output gates, one can easily obtain the degree of coupling much higher than unity. In other words, "biomolecular gears" are possible, and more than one step taken per ATP molecule hydrolized, observed in the case of the myosin II, is not an artefact.

The long-range shortcuts give the network small-world properties, characteristic for the dynamics of partly unfolded proteins. The structure of the myosin II is similar to that of small G proteins, e.g., the protein Ras (rat sarcoma) p21, both classes of proteins having a common ancestor [86]. Both in the Ras protein [15,87] and in the myosin II [88–91], one of the α helices unwinds in part after binding the nucleoside triphosphate, which makes the neighboring region partly disordered, and thus fluctuating and flexible. The detachment of the motor molecule from its track corresponds to the attachment of the signal transducting G protein to its effector. As a consequence, taking several steps per ATP molecule hydrolyzed by myosin II could correspond to the activation of many effectors per GTP molecule hydrolyzed by a malignantly mutated oncogene Ras protein. Also, in the transcription factor p53, the DNA binding core domain is partly disordered [92]. The commonly assumed model of facilitated, alternating three- and one-dimensional passive diffusion does not explain all the known facts concerning the search for a proper binding site on the DNA [93], so a hypothesis that this search can be active, using the free energy of a single ATP molecule hydrolysis many times, seems reasonable.

Nevertheless, the degree of coupling for most protein machines is lower than or equal to unity. Simultaneously, most protein enzymes display the Michaelis-Menten dependence of the asymptotic fluxes on the substrate concentration. Gating the reactions by single pairs of conformational transition substates is a sufficient condition for the conformationally fluctuating enzymes to obey the Michaelis-Menten kinetics [5,41]. There are, thus, solid grounds to suppose that the theory presented in Sec. III is applicable in the description of action of most biological machines. Doubts can be settled via an analysis of the time correlation functions of the noise, observed in appropriate single-molecule experiments [56,64].

Of course, networks with gates comprising single transition substates should only be treated as effective. The actual networks of conformational transitions are certainly much more complex. Various networks and systems of gates lead to the same or similar values of the quantities $\tau_{\rm M}(l_0 \leftrightarrow \{l,l'\})$ in the expressions for the slippage functions $W_i(A_i)$. Similarly, various networks make identical predictions of the statistical properties of the dichotomous noise observed [60,61]. It is a task for theoreticians to propose an algorithm of constructing the minimum effective networks that interpret the flux-force characteristics of the particular classes of protein machines.

We stated a hypothesis that the protein conformational transition networks, as just as higher-level biological networks, the protein interaction network, and the metabolic network, have evolved in a process of self-organized criticality. A proposal follows from this to adopt evolving scale-free trees as universal models of conformational transition networks in biomolecular machines. To reconstruct the funnel-like temperature dependence of the network architecture, an appropriately chosen temperature variation of transition probabilities has to be considered. We assumed that the free energy-donating reaction (usually the ATP hydrolysis) is singly gated and proceeds through the main hubs. In fact, the dependence of both the input and the output fluxes on the ATP concentration found in our simulations is of Michaelis-Menten form, which agrees with many experiments. The universality of the ATP hydrolysis is to be confronted with the fact that the main hubs are very stable and evolve slowly. On the other hand, nodes with low connectivity evolve faster and can be fitted evolutionarily, being good candidates for, if need be, either single or multiple exit gates of the free energy-accepting process.

ACKNOWLEDGMENTS

This study has been supported in part by the Polish Ministry of Science and Higher Education (Project No. N202 180038). M.T. additionally thanks the Foundation for Polish Science for support through a FOCUS fellowship.

APPENDIX: STATIONARY FLUXES AND MEAN FIRST-PASSAGE TIMES

Let $\mathbf{S}$ be an arbitrary set of states of a certain system with stochastic dynamics determined by a system of master equations such as (1). The set $\mathbf{S}$ can be considered as a network (diagram or graph): the states are the nodes (vertexes) and the nonzero transitions correspond to the links (edges). Following Hill's algorithm [43], the stationary occupation probability of a state l is

$$p_l = \frac{D_l(\mathbf{S})}{D(\mathbf{S})}, \tag{A1}$$

where $D_l(\mathbf{S})$ denotes the sum of products of transition probabilities in all appropriately constructed directional diagrams for the state l, and

$$D(\mathbf{S}) = \sum_{l\in\mathbf{S}} D_l(\mathbf{S}). \tag{A2}$$

Knowing the stationary occupation probabilities of distinguished substates in the kinetic schemes presented in Figs. 1 and 2, we can determine all the stationary fluxes in which we are interested. These appear to be related to the appropriate mean first-passage times.

To find the mean first-passage time from some initial to some final state of the diagram $\mathbf{S}$, one has to put a statistical ensemble of the systems into the initial state, observe the times needed by them to reach the final state, and average the result. But one can also consider some equivalent infinite process for a single system, assuming that each time a given system reaches the final state, the same system appears anew at the initial state. This corresponds to a modification of the diagram $\mathbf{S}$, consisting in a redirection of the final transition to the initial state combined with a simultaneous elimination of the final state. After a long enough time, this will be the reciprocal stationary flux in the modified diagram, which determines the presumed mean first-passage time. This stationary flux can be calculated with the help of the Hill algorithm.

In the case of equilibrium diagrams, with the detailed balance condition satisfied for all states, a cut out of any subdiagram $\mathbf{M}$ in $\mathbf{S}$ does not change the probability fluxes, so that using the notion of the conditional probability, one can replace Eq. (A1) by a more general equation

$$p_l = \frac{D_l(\mathbf{M})}{D(\mathbf{M})} P^{\mathrm{eq}}(\mathbf{M}), \tag{A3}$$

where $P^{\mathrm{eq}}(\mathbf{M})$ is the equilibrium occupation probability of the subset of states $\mathbf{M}$. In Ref. [41], we showed that the mean first-passage time from the state l_0 to l in the equilibrium diagram $\mathbf{M}$ can be expressed with the help of only the quantities $D_l(\mathbf{M})$ for the unmodified diagram $\mathbf{M}$:

$$\tau_{\mathbf{M}}(l_0 \to l) = \sum_{\mathbf{M}_{l_0}\cup\mathbf{M}_l} \frac{D_l(\mathbf{M}_l) D(\mathbf{M}_{l_0})}{D_l(\mathbf{M})}. \tag{A4}$$

Above, the summation runs over all the possible dissections $\mathbf{M}_{l_0} \cup \mathbf{M}_l$ of $\mathbf{M}$, the subdiagram $\mathbf{M}_{l_0}$ containing the site l_0 and the subdiagram $\mathbf{M}_l$ containing the site l.

The formula (A4) is very useful in making it possible to decompose any mean first-passage time into two components:

$$\tau_{\mathbf{M}}(l_0 \to l) = \sum_{\mathbf{M}_{l_0}\cup\mathbf{M}_{ll'}} \frac{D_l(\mathbf{M}_{ll'}) D(\mathbf{M}_{l_0})}{D_l(\mathbf{M})} + \sum_{\mathbf{M}_{l_0l'}\cup\mathbf{M}_l} \frac{D_l(\mathbf{M}_l) D(\mathbf{M}_{l_0l'})}{D_l(\mathbf{M})} \tag{A5}$$

for an arbitrary state $l' \in \mathbf{M}$ different both from l_0 and l. In the dissection $\mathbf{M}_{l_0} \cup \mathbf{M}_{ll'}$, the subdiagram $\mathbf{M}_{l_0}$ contains l_0 but not l and l', and the subdiagram $\mathbf{M}_{ll'}$ contains l and l' but not l_0. Conversely, in the dissection $\mathbf{M}_{l_0l'} \cup \mathbf{M}_l$, the subdiagram $\mathbf{M}_{l_0l'}$ contains l_0 and l' but not l, and the subdiagram $\mathbf{M}_l$ contains l but not l_0 and l'. Note that in the first component in Eq. (A5), l' can be exchanged with l, whereas in the second component, l' can be exchanged with l_0. Consequently, it is worth rewriting Eq. (A5) in the form

$$\tau_{\mathbf{M}}(l_0 \to l) = \tau_{\mathbf{M}}(l_0 \to \{l,l'\}) + \tau_{\mathbf{M}}(\{l_0,l'\} \to l). \tag{A6}$$

Here, $\tau_{\mathbf{M}}(l_0 \to \{l,l'\})$ has a direct meaning of the mean first-passage time from l_0 to l or l'. The interpretation of $\tau_{\mathbf{M}}(\{l_0,l'\} \to l)$ is more troublesome and was imprecise in Ref. [41]. However, we can always treat $\tau_{\mathbf{M}}(\{l_0,l'\} \to l)$ as a completion of $\tau_{\mathbf{M}}(l_0 \to \{l,l'\})$ to $\tau_{\mathbf{M}}(l_0 \to l)$.

Let us define the sum of the forward and reverse mean first-passage times:

$$\tau_{\mathbf{M}}(l_0 \leftrightarrow l) = \tau_{\mathbf{M}}(l_0 \to l) + \tau_{\mathbf{M}}(l \to l_0). \tag{A7}$$

With the help of Eq. (A3), it can be expressed as

$$\tau_{\mathbf{M}}(l_0 \leftrightarrow l) = D(\mathbf{M}) \sum_{\mathbf{M}_{l_0}\cup\mathbf{M}_l} \frac{D_l(\mathbf{M}_l) D_{l_0}(\mathbf{M}_{l_0})}{D_l(\mathbf{M}) D_{l_0}(\mathbf{M})}. \tag{A8}$$

The symmetrical counterpart of Eq. (A6) reads

$$\tau_{\mathbf{M}}(l_0 \leftrightarrow l) = \tau_{\mathbf{M}}(l \leftrightarrow \{l_0,l'\}) + \tau_{\mathbf{M}}(l_0 \leftrightarrow \{l,l'\}). \tag{A9}$$

From the symmetry enabling us to write Eq. (21) in an alternative form, a useful relation can be derived:

$$\tau_{\mathbf{M}}(l_0 \leftrightarrow \{l,l'\}) - \tau_{\mathbf{M}}(l_0 \leftrightarrow \{l,l''\}) = \tau_{\mathbf{M}}(l \leftrightarrow \{l_0,l''\}) - \tau_{\mathbf{M}}(l \leftrightarrow \{l_0,l'\}). \tag{A10}$$

It ensures that the expression under the logarithm in Eq. (15) will be positive irrespective of the sign of W_i, and it appears to be important in the proof that for single input and output gates the modulus of the degree of coupling can never exceed unity.

The continuation of the reasoning applied in the derivation of Eq. (A6) results in the relation

$$\tau_{\mathbf{M}}(l_0 \to \{l,l'\}) = \tau_{\mathbf{M}}(\{l_0,l''\} \to \{l,l'\}) + \tau_{\mathbf{M}}(l_0 \to \{l,l',l''\}) \tag{A11}$$

and its symmetrical counterpart. From that, another useful relation follows:

$$\tau_{\mathbf{M}}(l_0 \leftrightarrow \{l,l'\}) - \tau_{\mathbf{M}}(l_0 \leftrightarrow \{l,l''\}) = \tau_{\mathbf{M}}(l' \leftrightarrow \{l'',l_0\}) - \tau_{\mathbf{M}}(l' \leftrightarrow \{l''l\}), \tag{A12}$$

which is important in the discussion of Eq. (17) in the main text.

[1] M. Kurzynski, *The Thermodynamic Machinery of Life* (Springer, Berlin, 2006).
[2] H. Frauenfelder, S. G. Sligar, and P. G. Wolynes, Science **254**, 1598 (1991).
[3] A. E. García, R. Blumenfeld, G. Hummer, and J. A. Krumhansl, Physica D **107**, 225 (1997).
[4] A. Kitao, S. Hayward, and N. Go, Proteins **33**, 496 (1998).
[5] M. Kurzynski, Prog. Biophys. Mol. Biol. **69**, 23 (1998).
[6] H. Frauenfelder, *The Physics of Proteins: An Introduction to Biological Physics and Molecular Biophysics* (Springer, Berlin, 2010).
[7] K. Henzler-Wildman and D. Kern, Nature (London) **450**, 964 (2007).
[8] S. Yang, N. K. Banavali, and B. Roux, Proc. Natl. Acad. Sci. (USA) **106**, 3776 (2009).
[9] P. Bernado and M. Blackledge, Nature (London) **468**, 1046 (2010).
[10] A. F. Fink, Curr. Opin. Struct. Biol. **15**, 35 (2005).
[11] V. N. Uversky and A. K. Dunker, Biochim. Biophys. Acta **1804**, 1231 (2010).
[12] T. Chouard, Nature (London) **471**, 151 (2011).
[13] K. Lindorff-Larsen, R. B. Best, M. A. DePristo, C. M. Dobson, and M. Vendruscolo, Nature (London) **433**, 128 (2005).
[14] H. Heise, S. Luca, B. de Groot, H. Grubmüller, and M. Baldus, Biophys. J. **89**, 2113 (2005).
[15] Y. Arai, A. H. Iwane, T. Wazawa, H. Yokota, Y. Yshii, T. Kataoko, and T Yanagida, Biochem. Biophys. Res. Commun. **343**, 809 (2006).
[16] M. Vendruscolo, Curr. Opin. Struct. Biol. **17**, 15 (2007).
[17] A. Shehu, L. E. Kavraki, and C. Clementi, Biophys. J. **92**, 1503 (2007).
[18] S. Wu, P. I. Zhuravlev, and G. A. Papoian, Biophys. J. **95**, 5524 (2008).
[19] P. Senet, G. G. Maisuradze, C. Foulie, P. Delarue, and H. A. Scheraga, Proc. Natl. Acad. Sci. (USA) **104**, 19708 (2008).
[20] N. Furnham, T. L. Blundel, M. A. DePristo, and T. C. Terwilliger, Nat. Struct. Mol. Biol. **13**, 184 (2006).
[21] P. V. Burra, Y. Zhang, A. Godzik, and B. Stec, Proc. Natl. Acad. Sci. (USA) **106**, 10505 (2009).
[22] F. Rao and A. Caflisch, J. Mol. Biol. **342**, 299 (2004).
[23] S. V. Krivov and M. Karplus, Proc. Natl. Acad. Sci. (USA) **101**, 14766 (2004).
[24] G. J. Rylance, R. L. Johnston, Y. Matsunaga, C.-B. Li, A. Baba, and T. Komatsuzaki, Proc. Natl. Acad. Sci. (USA) **103**, 18551 (2006).
[25] B. Baba and T. Komatsuzaki, Proc. Natl. Acad. Sci. (USA) **104**, 19297 (2007).
[26] D. Gfeller, P. De Los Rios, A. Caflisch, and F. Rao, Proc. Natl. Acad. Sci. (USA) **104**, 1817 (2007).
[27] F. Noe and S. Fischer, Curr. Opin. Struct. Biol. **18**, 154 (2008).
[28] A. Enosh, B. Raveh, O. Furman-Schueler, D. Halperin, and N. Ben-Tal, Biophys. J. **95**, 3850 (2008).
[29] C. K. Materese, C. C. Goldmon, and G. Papoian, Proc. Natl. Acad. Sci. (USA) **105**, 10659 (2008).
[30] D. J. Wales, Curr. Opin. Struct. Biol. **20**, 3 (2010).
[31] C.-S. Goh, D. Milburn, and M. Gerstein, Curr. Opin. Struct. Biol. **14**, 104 (2004).
[32] A. Vologodskii, Phys. Life Rev. **3**, 119 (2006).
[33] K. Okazaki and S. Takada, Proc. Natl. Acad. Sci. (USA) **105**, 11182 (2008).
[34] O. L. Lange, N. A. Lakomek, C. Farés, G. F. Schröder, K. F. A. Walter, S. Becker, J. Meiler, H. Grubmüller, C. Griesinger, and G. L. de Groot, Science **320**, 1475 (2008).
[35] I. Bahar, C. Chennubhotla, and D. Tobi, Curr. Opin. Struct. Biol. **17**, 633 (2007).
[36] Q. Cui and M. Karplus, Prot. Sci. **17**, 1295 (2008).
[37] R. G. Smock and L. M. Gierasch, Science **324**, 198 (2009).
[38] B. Widom, Science **148**, 1555 (1965).
[39] S. H. Northrup and J. T. Hynes, J. Chem. Phys. **73**, 2700 (1980).
[40] R. Zwanzig, Acc. Chem. Res. **23**, 148 (1990).
[41] M. Kurzynski and P. Chelminiak, J. Stat. Phys. **110**, 137 (2003).
[42] L. A. Blumenfeld, *Problems of Biological Physics* (Springer, Berlin, 1982) (English translation from 1974 Russian edition).
[43] T. L. Hill, *Free Energy Transduction and Biochemical Cycle Kinetics* (Springer, New York, 1989).
[44] K. Kitamura, M. Tokunaga, A. H. Iwane, and T. Yanagida, Nature (London) **397**, 129 (1999).
[45] K. Kitamura, M. Tokunaga, S. Esaki, A. H. Iwane, and T. Yanagida, Biophysics **1**, 1 (2005).
[46] M. Nishikawa, H. Takagi, T. Shibata, A. H. Iwane, and T. Yanagida, Phys. Rev. Lett. **101**, 128103 (2008).
[47] X. Liu and G. H. Pollack, Biophys. J. **86**, 353 (2004).
[48] H. Kojima, M. Kikumoto, H. Sakakibara, and K. Sakakibara, J. Biol. Phys. **28**, 335 (2002).
[49] R. Mallik, B. C. Carter, S. A. Lex, S. J. King, and S. P. Gross,, Nature (London) **427**, 649 (2004).
[50] S. L. Reck-Peterson, A. Yildiz, A. P. Carter, A. Gennerich, N. Zhang, and R. D. Vale, Cell **126**, 335 (2006).
[51] T. Shima, T. Kon, K. Imamula, R. Ohkura, and K. Sutoh, Proc. Natl. Acad. Sci. (USA) **103**, 17736 (2006).
[52] R. D. Astumian, Science **276**, 917 (1997).
[53] F. Jülicher, A. Ajdari, and J. Prost, Rev. Mod. Phys. **69**, 1269 (1997).
[54] M. E. Fisher and A. B. Kolomeisky, Proc. Natl. Acad. Sci. (USA) **96**, 6597 (1999).
[55] H. Wang and G. Oster, Nature (London) **396**, 279 (1998).
[56] H. P. Lu, L. Xun, and X. S. Xie, Science **282**, 1877 (1998).
[57] L. Edman and R. Rigler, Proc. Natl. Acad. Sci. (USA) **97**, 8266 (2000).
[58] O. Flomenbom, K. Velonia, D. Loss, S. Masuo, M. Cotlet, Y. Engelborghs, J. Hofkens, A. E. Rowan, R. J. M. Nolte, M. van der Auweraer, F. C. de Schryver, and J. Klafter, Proc. Natl. Acad. Sci. (USA) **102**, 2368 (2005).
[59] O. Flomenbom, J. Klafter, and A. Szabo, Biophys. J. **88**, 3780 (2005).
[60] W. J. Bruno, J. Yang, and J. E. Pearson, Proc. Natl. Acad. Sci. (USA) **102**, 6326 (2005).
[61] O. Flomenbom and R. J. Silbey, Proc. Natl. Acad. Sci. (USA) **103**, 10907 (2006).
[62] B. P. English, W. Min, A. M. van Oijen, K. T. Lee, G. Luo, H. Sun, B. J. Cherayil, S. C. Kou, and X. S. Xie, Nature Chem. Biol. **2**, 87 (2006).
[63] M. Morimatsu, T. Kakagi, G. K. Ota, R. Iwamoto, T. Yanagida, and Y. Sato, Proc. Natl. Acad. Sci. (USA) **104**, 18013 (2007).
[64] M. Kurzynski, Cell. Mol. Biol. Lett. **13**, 502 (2008).
[65] T. P. Terada, M. Sasai, and T. Yomo, Proc. Natl. Acad. Sci. (USA) **99**, 9202 (2002).

[66] E. W. Montroll and B. J. West, in *Fluctuation Phenomena*, edited by E. W. Montroll and J. L. Lebowitz (North-Holland, Amsterdam, 1987), p. 61.
[67] P. Bak and K. Sneppen, Phys. Rev. Lett. **71**, 4083 (1993).
[68] P. Bak, *How Nature Works: The Science of Self-Organized Criticality* (Copernicus, New York, 1996).
[69] K. Sneppen and G. Zocchi, *Physics in Molecular Biology* (Cambridge University Press, New York, 2005).
[70] A.-L. Barabási and R. Albert, Science **286**, 509 (1999).
[71] R. Albert and A.-L. Barabási, Rev. Mod. Phys. **74**, 47 (2002).
[72] H. Jeong, B. Tombor, R. Albert, Z. N. Oltvai, and A.-L. Barabási, Nature (London) **407**, 651 (2000).
[73] H. Jeong, S. P. Mason, A.-L. Barabási, and Z. N. Oltvai, Nature (London) **411**, 41 (2001).
[74] E. Ravasz, A. L. Somera, D. A. Omgru, Z. N. Oltvai, and A.-L. Barabási, Science **297**, 1551 (2002).
[75] C. Song, S. Havlin, and H. A. Makse, Nature (London) **433**, 392 (2005).
[76] J. P. K. Doye, Phys. Rev. Lett. **88**, 238701 (2002).
[77] N. Hori, G. Chikenji, R. S. Berry, and S. Takada, Proc. Natl. Acad. Sci. (USA) **106**, 73 (2009).
[78] I. A. Kovács, M. S. Szalay, and P Csermely, FEBS Lett. **579**, 2254 (2005).
[79] C. Böde, I. A. Kovács, M. S. Szalay, R. Palotai, T. Korcsmáros, and P. Csermely, FEBS Lett. **581**, 2776 (2007).
[80] D.-C. Ma, Y.-B. Diao, Y.-Z. Li, Y.-Z Guo, J. Wu, and M.-L. Li, Nat. Sci. **2**, 998 (2010).
[81] H. D. Rozenfeld, C. Song, and H. A. Makse, Phys. Rev. Lett. **104**, 025701 (2010).
[82] P. I. Zhuravlev and G. A. Papoian, Curr. Opin. Struct. Biol. **20**, 16 (2010).
[83] K.-I. Goh, G. Salvi, B. Kahng, and D. Kim, Phys. Rev. Lett. **96**, 018701 (2006).
[84] L. K. Gallos, C. Song, S. Havlin, and H. A. Makse, Proc. Natl. Acad. Sci. (USA) **104**, 7746 (2007).
[85] J. S. Kim, K.-I. Goh, G. Salvi, E. Oh, B. Kahng, and D. Kim, Phys. Rev. E **75**, 016110 (2007).
[86] F. J. Kull, R. D. Vale, and R. J. Fletterick, J. Muscle Res. Cell Motil. **19**, 877 (1998).
[87] I. Kosztin, R. Bruinsma, P. O'Lague, and K. Schulten, Proc. Natl. Acad. Sci. (USA) **99**, 3575 (2002).
[88] J. Xu and D. D. Root, Biophys. J. **79**, 1498 (2000).
[89] A. Houdussse and H. L. Sweeney, Curr. Opin. Struct. Biol. **11**, 182 (2001).
[90] L. K. Nitao, T. O. Yeates, and E. Reisler, Biophys. J. **83**, 2733 (2002).
[91] A. R. Thompson, N. Naber, C. Wilson, R. Cooke, and D. D. Thomas, Biophys. J. **95**, 5238 (2008).
[92] A. C. Joerger and A. R. Fersht, Annu. Rev. Biochem. **77**, 557 (2008).
[93] A. B. Kolomeisky, Phys. Chem. Chem. Phys. **13**, 2088 (2011).